Electronic Supplementary Material (ESI) for Faraday Discussions.

Supporting Information

Mechanistic Insights into C2 and C3 Product Generation Using Ni_3Al and Ni_3Ga Electrocatalysts for CO_2 Reduction

Aubrey R. Paris*, Andrew B. Bocarsly

**Correspondence: aparis@princeton.edu*

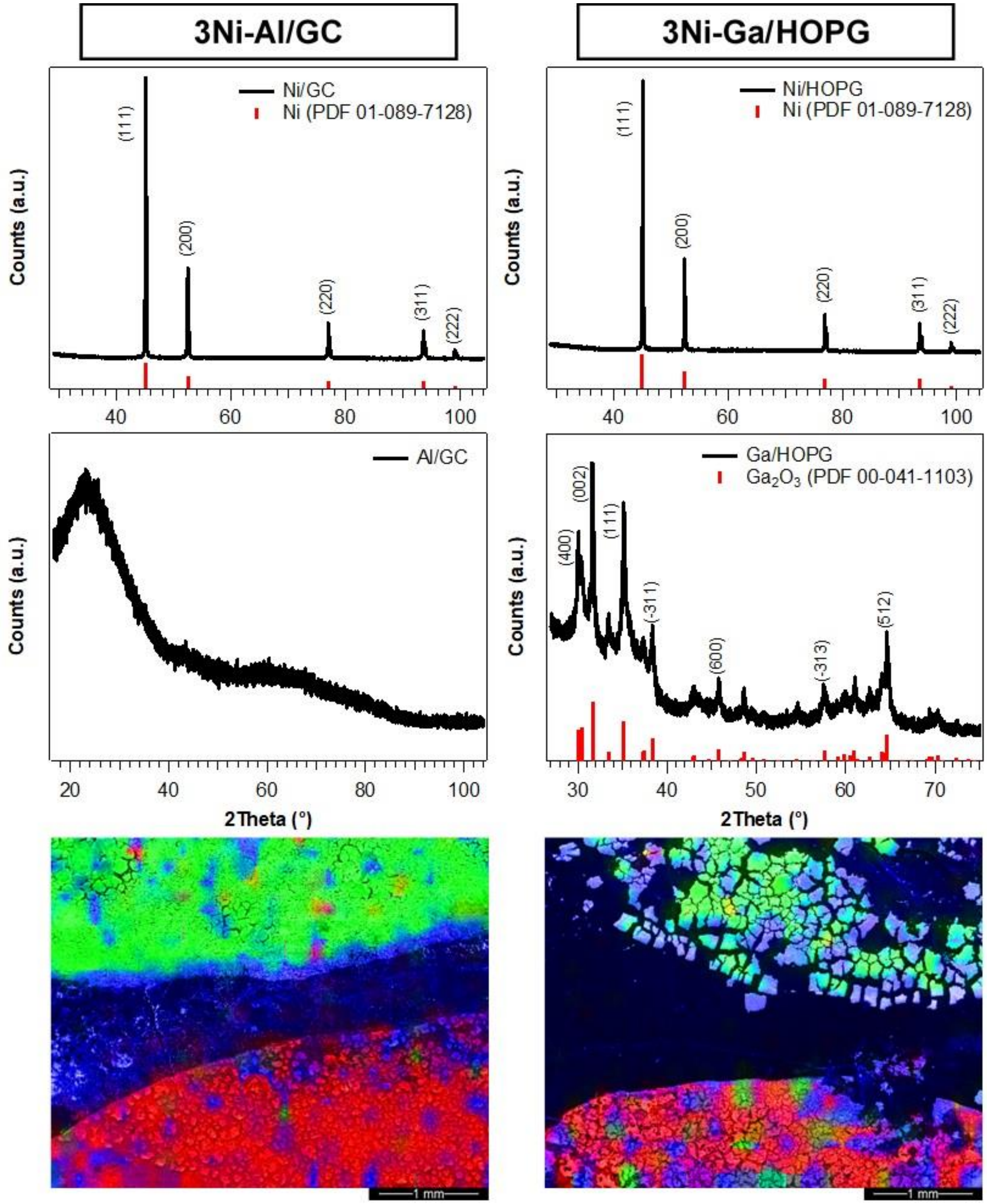

Figure S1. Additional materials characterization for 3Ni-Al/GC (left) and 3Ni-Ga/HOPG (right). XRD patterns (top, middle) indicate the presence of cubic Ni, amorphous Al, and monoclinic Ga_2O_3 (for clarity, only the most prominent Ga_2O_3 lattice planes are labeled). EDX maps (bottom) portray spatially isolated Ni (red) and Al or Ga (green) stripes; the carbon solid support is blue. EDX obtained using a 5 keV electron beam and ~12 mm working distance.

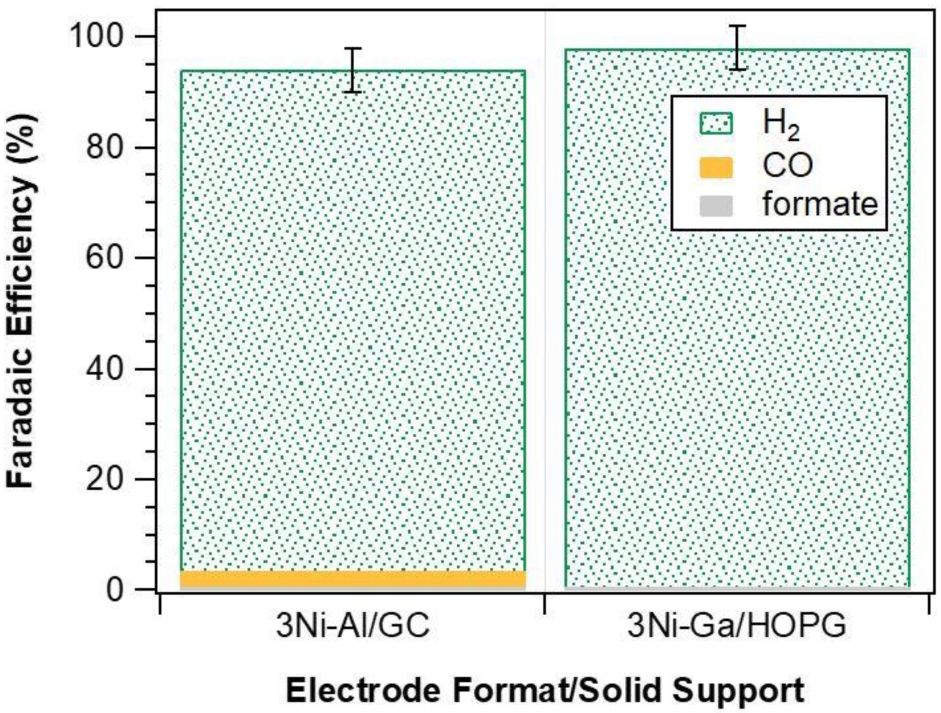

Figure S2. Sample Faradaic efficiency plots including the competitive product H_2, demonstrating charge balance. In this case, experiments using non-mixed 3Ni-Al/GC and 3Ni-Ga/HOPG electrodes primarily generated H_2 from the aqueous environment. Electrolysis experiments were conducted at –1.38 V vs. Ag/AgCl in pH 4.5, CO_2-saturated K_2SO_4 electrolyte. Subsequent electrolyses also achieved charge balance when considering H_2.

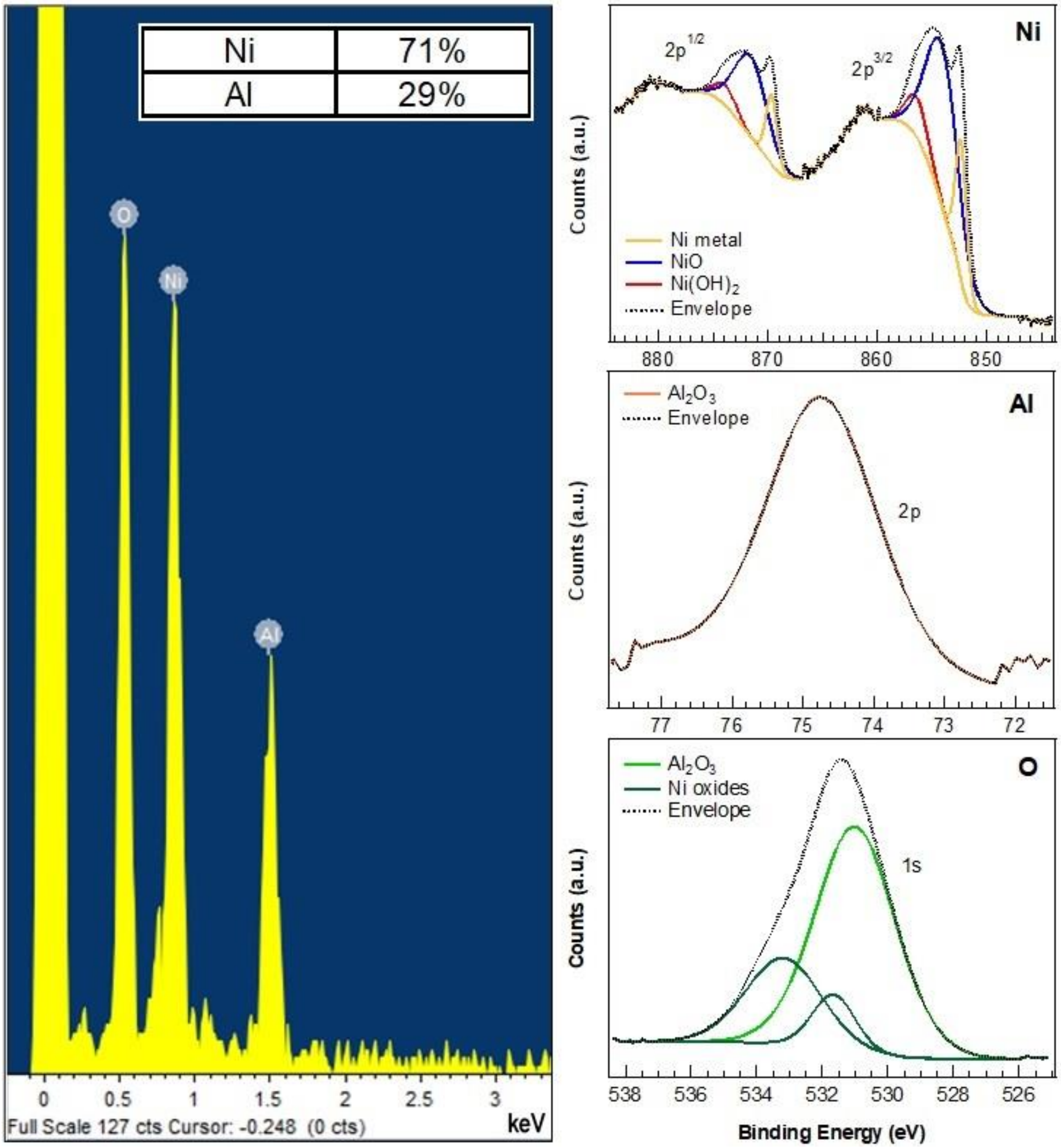

Figure S3. Additional materials characterization for Ni$_3$Al/HOPG. EDX spectroscopy (left) complements XRD data and confirms the nominal bulk stoichiometry. XPS spectra (right) point to a predominantly oxidized surface in which only a small portion of Ni is metallic. EDX obtained using a 5 keV electron beam and ~12 mm working distance.

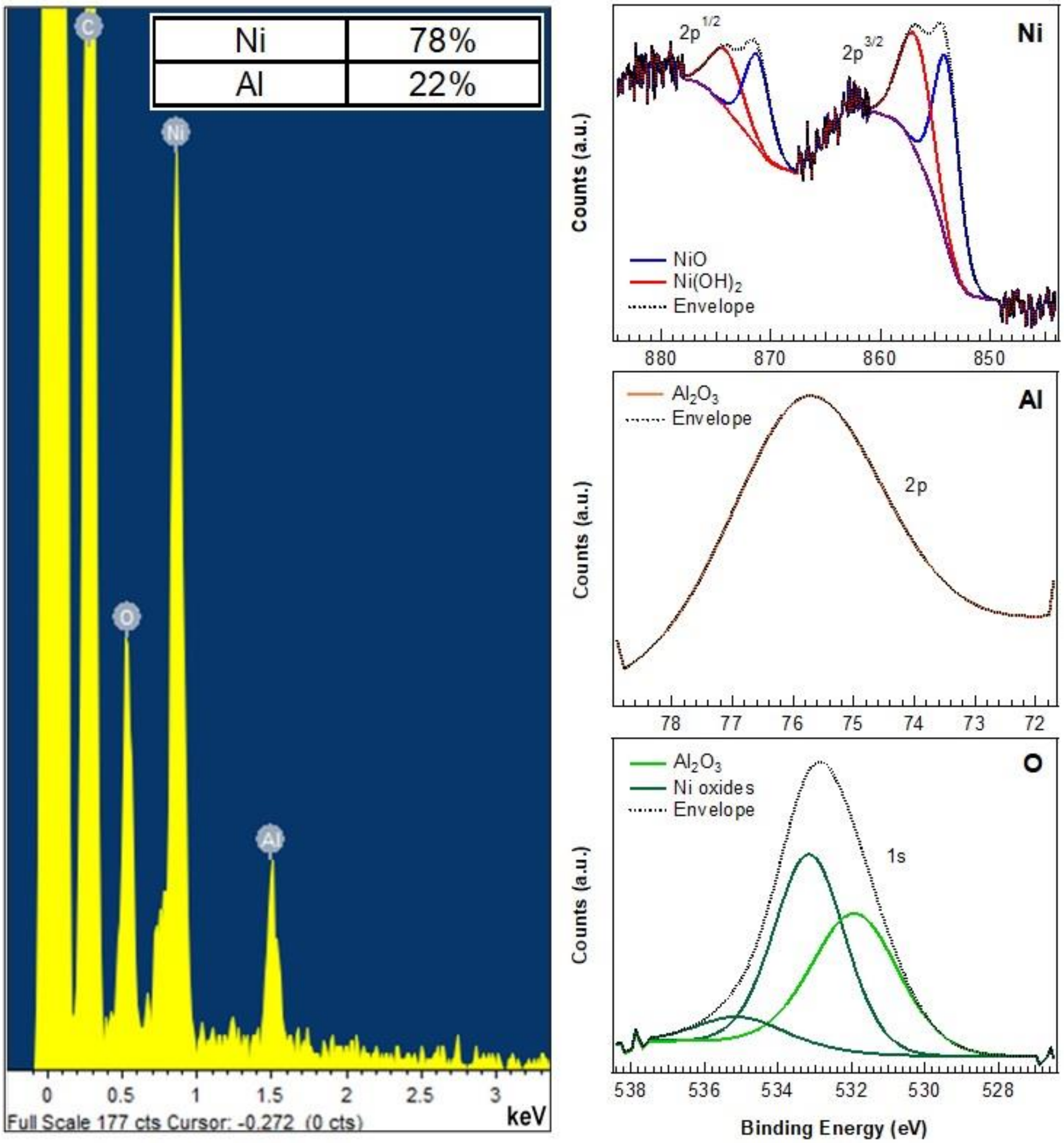

Figure S4. Additional materials characterization for Ni_3Al/RVC. EDX spectroscopy (left) complements XRD data and confirms the nominal bulk stoichiometry. XPS spectra (right) point to a completely oxidized surface when considering both Ni and Al. EDX obtained using a 5 keV electron beam and ~12 mm working distance.

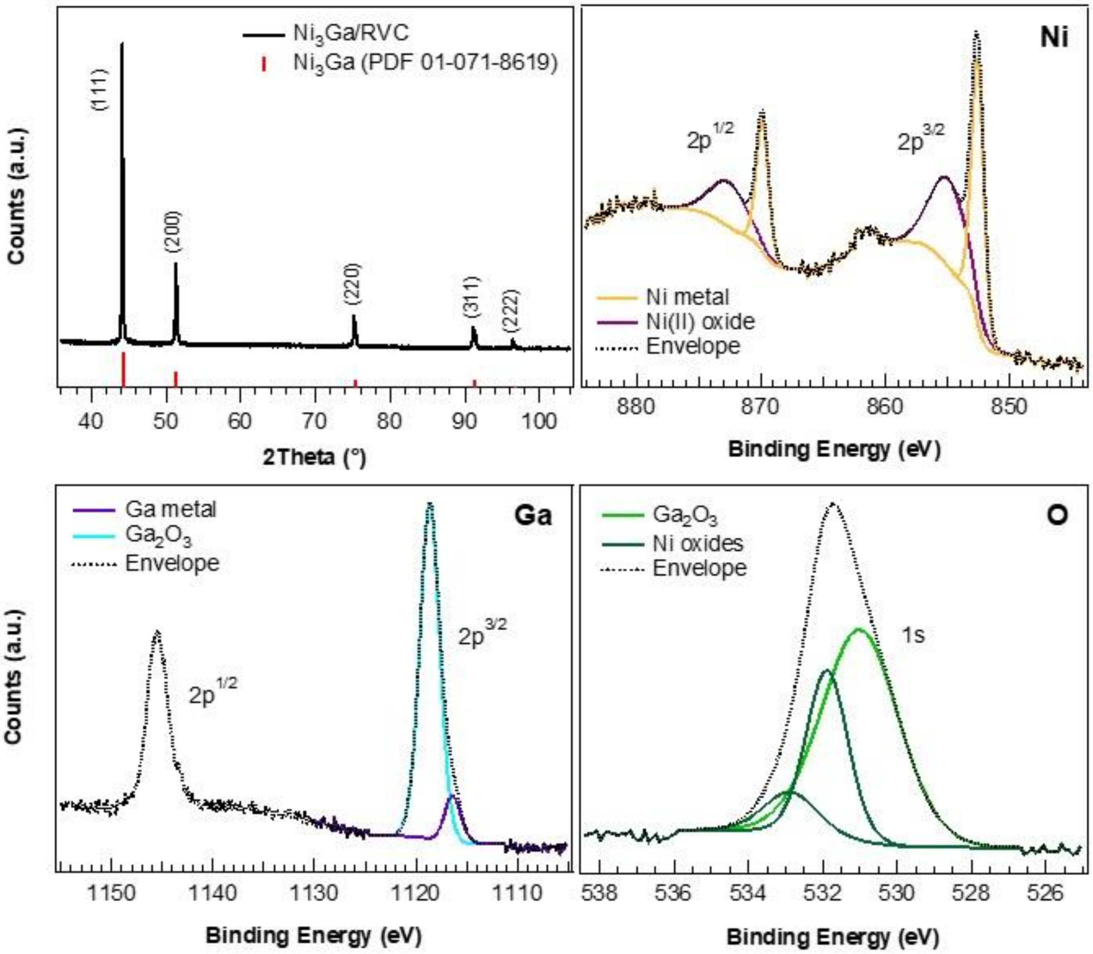

Figure S5. Bulk material and surface characterization of Ni_3Ga on RVC solid support. XRD (top left) confirms the nominal assignment, while XPS (top right; bottom) suggests that the surface of the film consists of a mixture of metallic and oxidized Ni and Ga. SEM images and EDX spectra for Ni_3Ga/RVC were previously reported.[1]

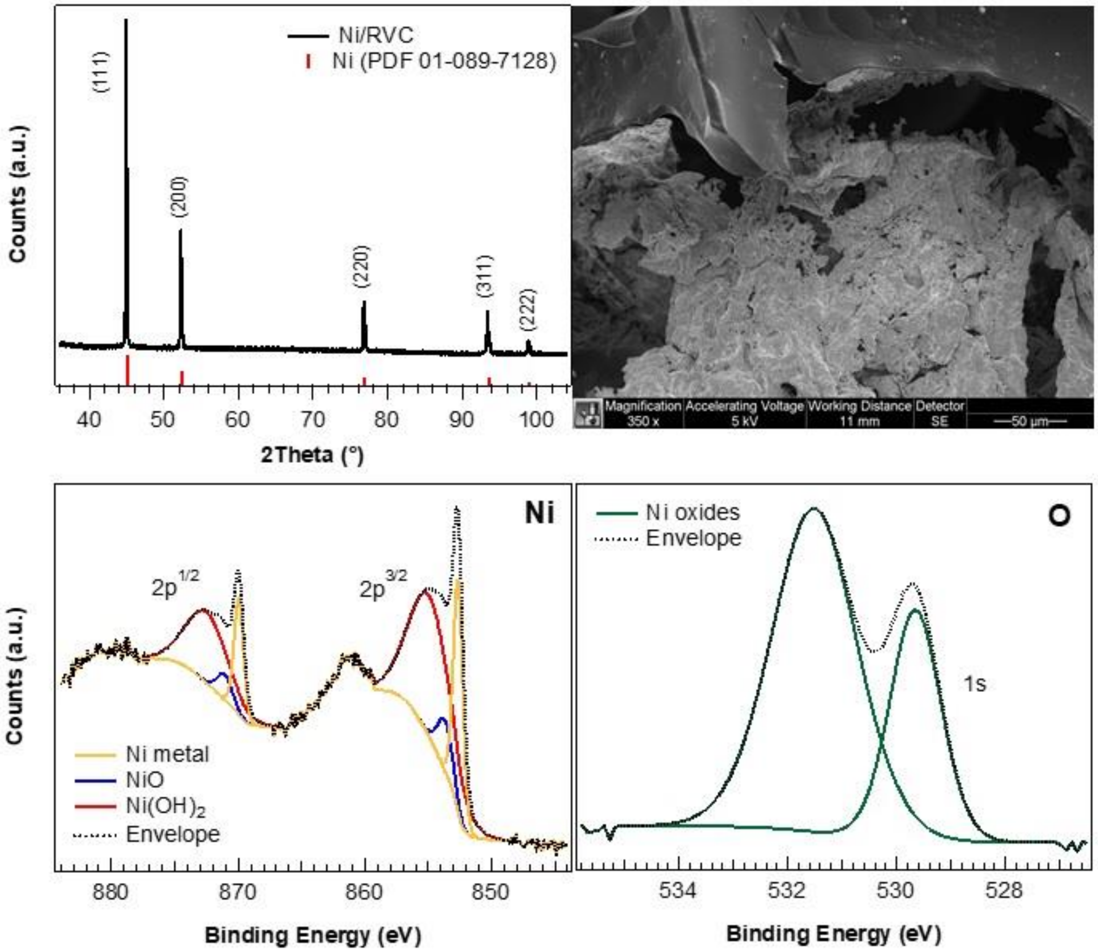

Figure S6. Materials characterization of the Ni half of 3Ni-Ga/RVC. XRD (top left) reveals that the bulk material consists of cubic Ni in the metallic state, while XPS data suggest that the surface is comprised of a mixture of metallic Ni and Ni(II) oxides (bottom). SEM imaging shows that Ni embedded within the porous carbon framework has a rough surface structure (top right), which diverges from the typical smooth platelet appearance of other materials deposited on RVC support.

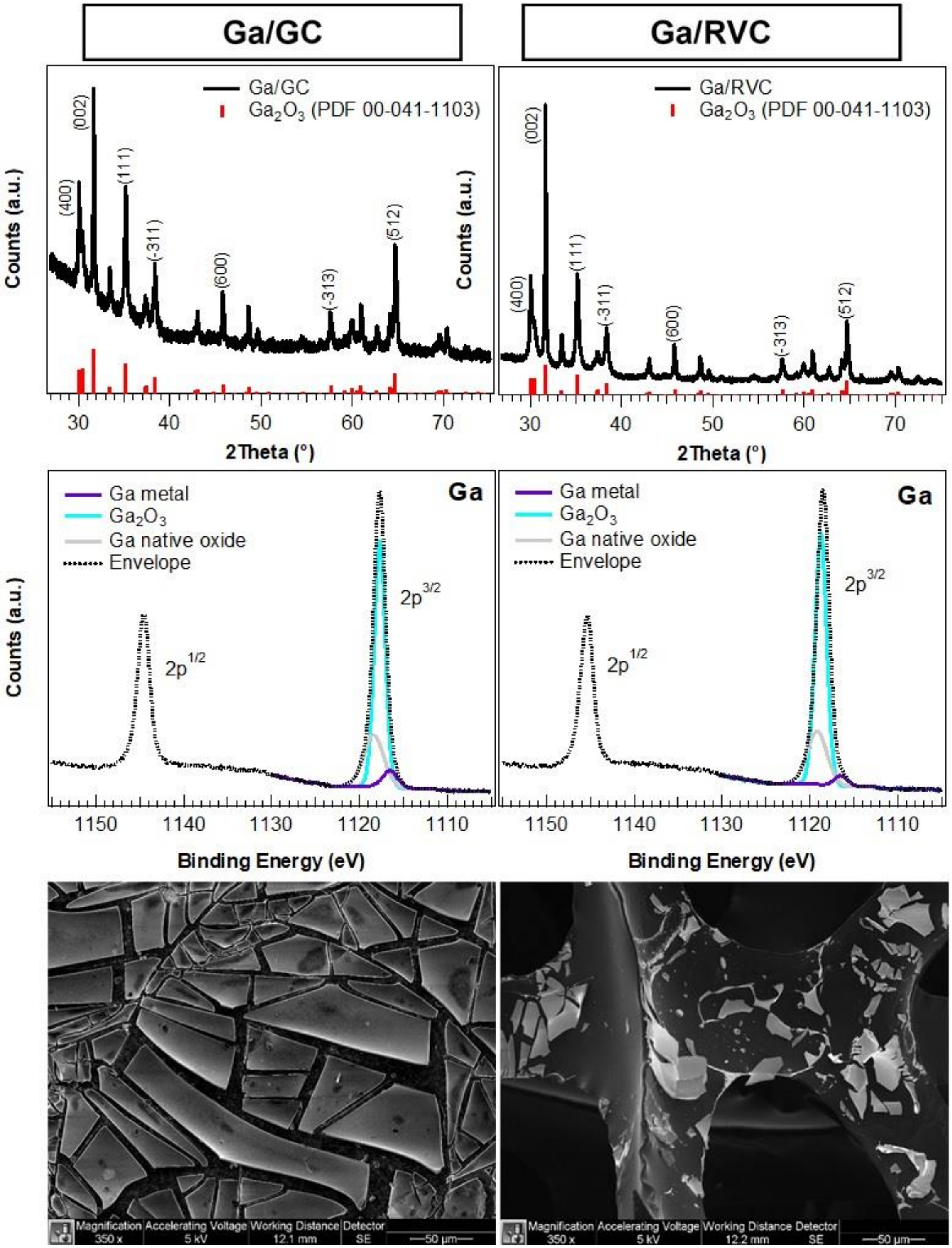

Figure S7. Materials characterization of the Ga halves of 3Ni-Ga/GC (left) and 3Ni-Ga/RVC (right). Per XRD analysis (top), both species are comprised of monoclinic Ga_2O_3, and XPS (middle) suggests that the surfaces are predominantly oxidized with minor contributions from Ga metal. SEM imaging (bottom) reveals that both Ga halves appear to be made up of flat platelet structures, a common morphological motif on both carbon supports.[1]

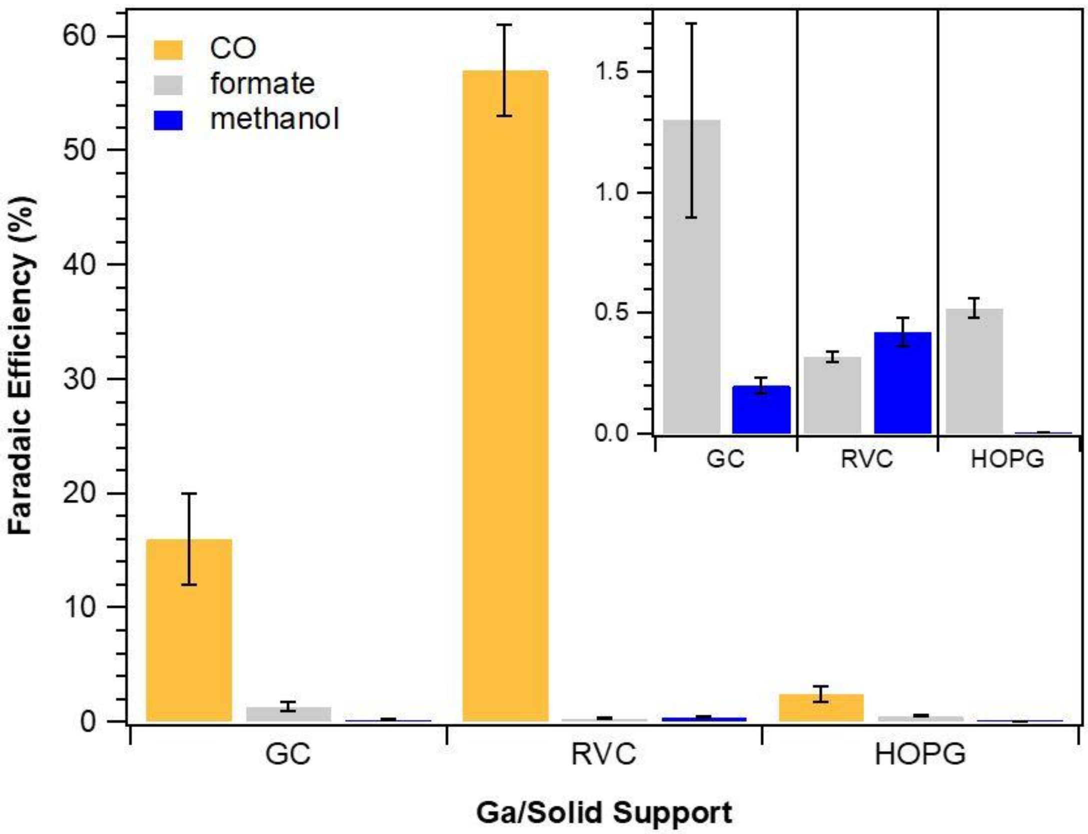

Figure S8. Faradaic efficiencies for CO_2 reduction products generated using Ga-based films (actual composition = monoclinic Ga_2O_3) on GC, RVC, and HOPG solid supports. While Faradaic efficiencies differ, product distribution remains constant. Electrolysis experiments were conducted at –1.38 V vs. Ag/AgCl in pH 4.5, CO_2-saturated K_2SO_4 electrolyte.

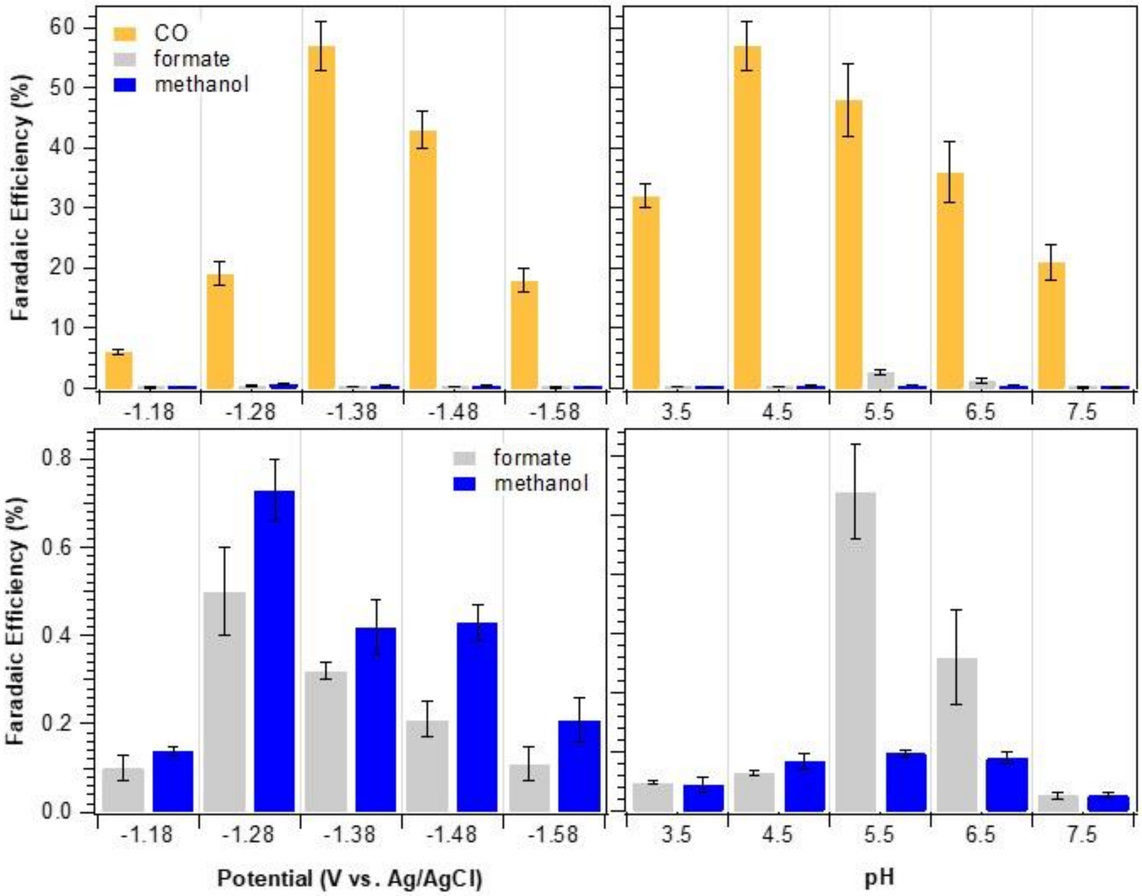

Figure S9. Faradaic efficiencies for CO_2 reduction products generated during potential (left) and pH (right) dependence experiments using Ga/RVC; the lower plots zoom-in on liquid-phase, minor products. CO, the major carbon-containing product, is maximized at –1.38 V vs. Ag/AgCl and pH 4.5 electrolyte, though high CO Faradaic efficiencies can be achieved across a range of conditions. Materials characterization suggests that the Ga films are comprised of monoclinic Ga_2O_3. For consistency, potential dependence experiments were conducted using pH 4.5, CO_2-saturated K_2SO_4 electrolyte, while pH dependence experiments utilized an operating potential of –1.38 V vs. Ag/AgCl.

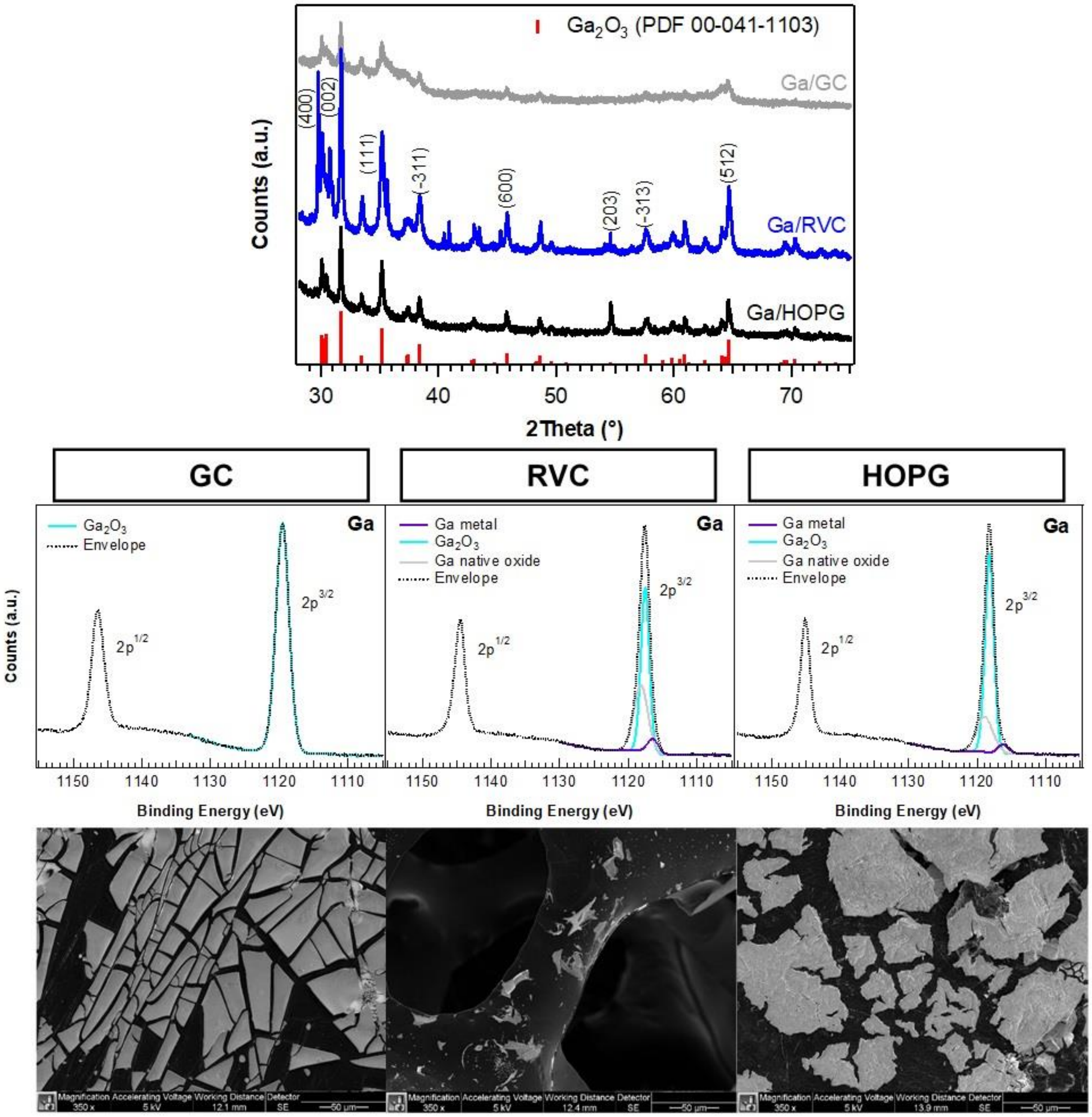

Figure S10. Post-electrolysis materials characterization of Ga drop-casted onto GC, RVC, and HOPG substrates. XRD (top; high-intensity peaks labeled for clarity) analysis suggests that the bulk films remain chemically stable, retaining their monoclinic Ga_2O_3 structure. XPS (middle) confirms surface stability, characterized by entirely or predominantly oxidized surfaces. SEM (bottom) imaging verifies morphological and physical stability on the carbon supports. Electrolysis experiments were conducted at –1.38 V vs. Ag/AgCl in pH 4.5, CO_2-saturated K_2SO_4 electrolyte.

Table S1. Electrolysis products achieved during single-metal control experiments on various carbon solid supports at –1.38 V vs. Ag/AgCl (0.1 M K_2SO_4, pH 4.5).

	CO			*formate*			*methanol*		
	HOPG	**GC**	**RVC**	**HOPG**	**GC**	**RVC**	**HOPG**	**GC**	**RVC**
Ni	0	1.7	27.7	0.02	0.01	0.06	0.01	0.01	0.06
Ga	2.4	16.5	56.7	0.5	1.3	0.3	0.005	0.2	0.4
Al	-	14.6	-	-	0.5	-	-	0	-

Table S2. Summary of carbon-containing products achieved during CO_2 reduction using each catalyst discussed herein. Electrolysis experiments were conducted at –1.38 V vs. Ag/AgCl in 0.1 M K_2SO_4 (pH 4.5).

Catalyst	*Faradaic Efficiency (H_2O Environment)*			*D_2O Environment*
	GC	**RVC**	**HOPG**	
Ni_3Al[*]	33% CO 1.9% 1-propanol 1.0% methanol 0.75% formate	33% CO 0.27% 1-propanol 0.22% methanol 0.18% formate	0.78% CO 0.34% 1-propanol 0.20% formate 0.15% methanol	49% CO (GC)
3Ni-Al	3.3% CO 0.3% formate	-	-	-
Ni_3Ga[†]	11.2% CO 0.23% formate 0.06% methanol	26% CO 1.0% formate 0.10% methanol	0.10% ethane	35% CO (GC) 3.3% CO (HOPG)
3Ni-Ga	6% CO 0.7% formate 0.045% methanol	52% CO 0.28% methanol 0.20% formate	0.075% formate	-
Ga[‡]	16% CO 1.3% formate 0.20% methanol	57% CO 0.42% methanol 0.32% formate	2.4% CO 0.52% formate 0.005% methanol	80% CO (RVC)

[*] GC data reported previously.[2]

[†] Data reported previously.[1]

[‡] XRD analysis suggests that Ga films employed in this study are comprised of monoclinic Ga_2O_3.

References

1 A. R. Paris, A. T. Chu, C. B. O'Brien, J. J. Frick, S. A. Francis and A. B. Bocarsly, *Journal of The Electrochemical Society*, 2018, **165**, H385–H392.
2 A. R. Paris and A. B. Bocarsly, *ACS Catalysis*, 2017, **7**, 6815–6820.